

# Effect of thermal stress, condensation and freezing–thawing action on the degradation of stones on the Castle of Chambord, France

Asaad Al-Omari · Xavier Brunetaud ·  
Kevin Beck · Muzahim Al-Mukhtar

Received: 21 April 2013 / Accepted: 28 August 2013 / Published online: 13 September 2013  
© Springer-Verlag Berlin Heidelberg 2013

**Abstract** This work consists in estimating the role of climatic conditions in the degradation of two French limestones, tuffeau and Richemont stone, used in the construction and the restoration of the Castle of Chambord, the largest castle in the Loire Valley, France. Meteorological data, air temperature, air relative humidity and rainfall were statistically analysed in combination with stone data from thermal–humidity sensors inserted into the walls. The climatic conditions of the surrounding area were described to assess their role in enhancing the degradation of the stones through three weathering processes: thermal stress, condensation and freezing–thawing. The damage risks due to the weathering processes were taken into account not only through the bulk effects on the stone surfaces, but also their effects were extended to investigate the damage that occurs within the porous structure of the stone. Field observations showed that the main patterns of degradation affecting the stones of the castle are biological colonization and stone detachment in the form of stone spalling and exfoliation. The results of the analysis show that there is no risk of damage to the stones due to thermal stress. Moreover, the two stones experience similar overall trends against freezing–thawing processes. Finally, this study clearly highlights the important role of condensation in the degradation of the stones of the castle.

**Keywords** Thermal stress · Condensation · Freezing–thawing · Weathering processes · Climatic conditions · Stonework

## Introduction

The main construction units for cultural-historic buildings, temples and monuments are stones. Moreover, stones have been used as an architectural feature, trim, ornament or facing for buildings or other structures. Pope et al. (2002) used the term cultural stones for “the stone that has been physically altered by humans—abraded, engraved, quarried, chipped or chiselled, or dressed”.

The preservation of historical monuments is not only considered as a cultural requirement, but also a scientific challenge; that is why, in the last few decades, considerable attention has been paid to studying the mechanisms that lead to the decay of built heritage and, therefore, to the stones used for construction. The weathering processes that cause monument degradation involve physical weathering due to mechanical stresses, such as stresses induced by freezing, thermal stress, salt crystallization and pollution. Moreover, chemical weathering results from changes in chemical and mineralogical composition. Finally, biological weathering, once triggered by the appropriate outdoor environment, including humid air and mild temperatures, promotes the growth of simple living organisms (e.g. fungi, lichen, bacteria and algae) on the outer surfaces of stones.

These weathering processes are related to the surrounding climatic conditions. In polar or hot desert environments, physical weathering processes may be considered to be the most common factors that control stone deterioration; in contrast, in the warm and wet regions, the effects of chemical and biological weathering processes are expected

A. Al-Omari · X. Brunetaud · K. Beck · M. Al-Mukhtar (✉)  
Universite d’Orléans, CNRS, CRMD FRE 3520, 1b rue de la  
Férollerie, 45071 Orleans Cedex 2, France  
e-mail: muzahim.al-mukhtar@univ-orleans.fr

A. Al-Omari  
Department of Civil Engineering, College of Engineering, Mosul  
University, Al-Majmooh Street, Mosul, Iraq

to be dominant. The effect of climatic and environmental conditions on the decay processes of stone building materials has already been the object of previous studies (Bonazza et al. 2009a, b; Camuffo and Sturaro 2001; Eklund 2008; Hoxha et al. 2010; Moropoulou et al. 1995; Ponziani et al. 2012; Van et al. 2007; Viles 2005).

The seasonal, daily and even hourly variations in climatic conditions, air temperature and air humidity play an important role in the decay of stone and could generate damage by fatigue. The estimation of damage risk related to the degradation of stones in the Castle of Chambord, due to the variation in climatic conditions through the weathering process of thermal stress, condensation and freezing–thawing action, has never before been studied. This paper aims to provide quantitative information that will help in understanding the degradation of two types of limestones, tuffeau and Richemont stone, used in the Castle of Chambord. The present work involves analysing meteorological elements together with the measured stone temperature and stone relative humidity in an attempt to assess the role of climatic conditions in the stones' degradation. Climatic conditions were analysed using data collected over more than 40 years from the meteorological station nearest to the castle and from a meteorological station installed on the roof of the east tower of the castle. The second set of data includes the measured stone temperature and relative humidity using thermal–humidity sensors inserted into the walls of the same tower. The study consists of not only observing the effects of weathering processes on the external surfaces of stone walls, but also in taking into account those processes that happen within the porous structure of the stone.

### The Castle of Chambord: site, stones and degradation of stones

The Castle of Chambord, built in 1519, is the largest castle in the Loire Valley, France, and has been part of the UNESCO World Heritage list since 2000. It is located in a rural area at a distance of about 50 km to the south-west of Orleans, at latitude 47°36'N, longitude 1°31'E, with an average elevation of about 84 m above sea level. This study is focused on the behaviour of stones located in the east tower, which has been only slightly restored and monitored for several years using thermal–humidity sensors and a weather station.

Tuffeau was the main building material used in the construction of not only the Castle of Chambord, but also many other French ancient buildings, including the famous castles of the Loire Valley. This soft limestone is very fragile and has low compressive strength. That is why a harder stone “Beauce limestone” was used for the

construction of the foundations of the castle (Janvier-Badosa et al. 2013). However, the particular properties of tuffeau, including its fine grain and its homogeneous white colour, meant it was commonly used for superstructures, including ornamented walls. During limited periods of the early twentieth century, the limestone named “Richemont stone” was used in the restoration of the tuffeau walls, where the degraded stones had to be replaced. For the east tower of the Castle of Chambord, tuffeau represents 80 % of the stones, whereas Richemont stone is limited to only 20 % (Janvier-Badosa et al. 2013). Neither tuffeau nor Richemont stone have a specific location on the walls of the castle.

The characterization of the studied stone was achieved using complementary laboratory techniques: X-ray diffraction tests (XRD), chemical analysis and thermo-gravimetric analysis (ATG), together with scanning electron microscopy (SEM). The pore size distribution was obtained by mercury intrusion porosimetry (MIP) testing. The engineering properties, Young's modulus, Poisson's ratio and unconfined compressive strength of the two stones in a dry state were measured using an Instron 4485 press machine. The thermal expansion of the stones was measured using a digital dial gauge. Moreover, the vacuum saturation method was used to measure the stones' physical properties; total porosity, dry density and skeleton density.

**Table 1** Main physical and thermo-hydro-mechanical properties of the two studied stones

Stone property	Stone type	
	Tuffeau	Richemont stone
Mineralogical composition	Calcite $\approx$ 50 %	Calcite $\approx$ 95 %
	Quartz $\approx$ 10 %	Quartz $\approx$ 5 %
	Opal	
	CT $\approx$ 30 %	
	Clays and micas $\approx$ 10 %	
Skeleton density ( $\text{g}/\text{cm}^3$ )	$2.57 \pm 0.01$	$2.71 \pm 0.01$
Bulk dry density ( $\text{g}/\text{cm}^3$ )	$1.30 \pm 0.02$	$1.94 \pm 0.01$
Total porosity (%)	$45.0 \pm 0.52$	$29.5 \pm 0.54$
Unconfined compressive strength (MPa)	$11.67 \pm 0.33$	$19.41 \pm 1.03$
Young modulus (MPa)	$3482 \pm 20$	$14962 \pm 233$
Poisson's ratio (%)	$0.207 \pm 0.005$	$0.231 \pm 0.004$
Linear thermal expansion coefficient ( $\text{K}^{-1}$ )	$(8.41 \pm 0.12)\text{E}-06$	$(5.84 \pm 0.04)\text{E}-06$
Water retention as a degree of saturation (%):		
33 % RH	2.63	0.42
56 % RH	3.62	0.68
76 % RH	6.81	1.55
98 % RH	22.89	3.94

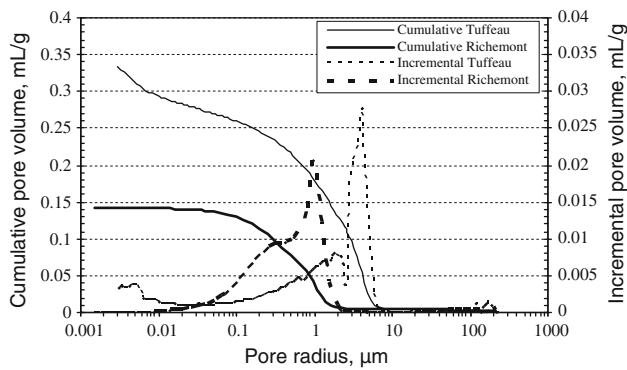


**Fig. 1** Pore size distribution for the two studied stones

Table 1 summarizes all the measured physical and thermo-hydro-mechanical properties of the two stones.

In the present work, the two porous limestones, tuffeau and Richemont stone, used in the construction and conservation of the Castle of Chambord are considered. Tuffeau is composed of calcite, quartz, opal (cristobalite/tridymite) and clay–mica minerals, while the Richemont stone is mainly composed of calcite with a low percentage of quartz. Figure 1 shows the results of porosimetry: the tuffeau matrix is composed of a wide range of pore access radii, between 0.003 μm and 10 μm, while they are between 0.01 and 2 μm for Richemont stone. Tuffeau, white-light beige in colour, and Richemont stone, light beige, are greenish and reddish in colour, respectively, after wetting. Tuffeau is a lightweight material with high total porosity compared with Richemont stone.

The two stones differ in terms of the clay mineral content and the fineness of the pores, explaining the different amounts of moisture absorbed by the stones when exposed to high humidity conditions. The degrees of saturation of tuffeau and Richemont stone resulting from

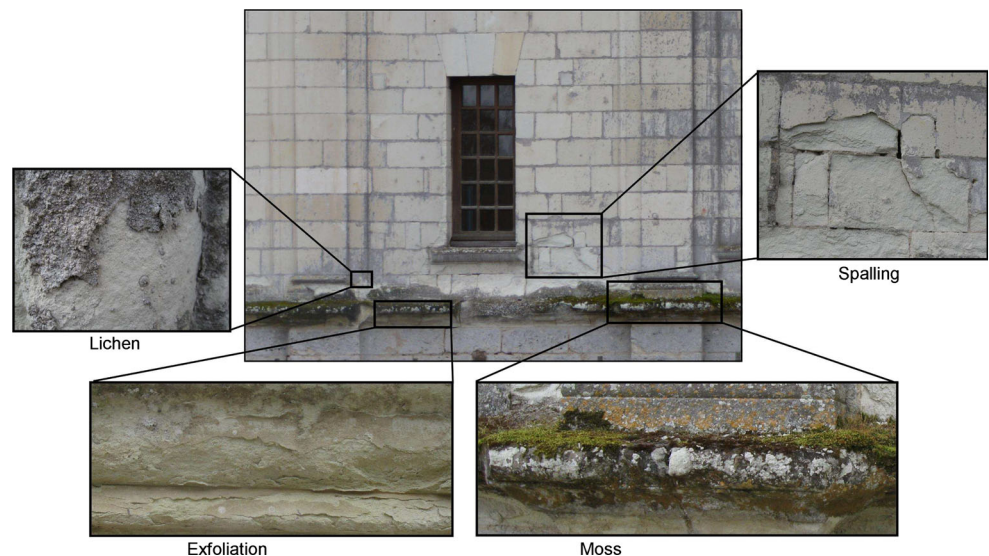
exposure at different relative humidities are given in Table 1. The water retention capacity of tuffeau is always much higher than that of Richemont stone. This suggests that tuffeau may be more subjected to degradation due to water transport than Richemont stone.

Several studies concerning the Castle of Chambord were carried out: either from the perspective of historical study (Janvier-Badosa et al. 2013), to identify the types of stone degradation (Beck and Al-Mukhtar 2005; Janvier-Badosa et al. 2010) or for the scientific monitoring and planning of restoration works using new digital techniques (Brunetaud et al. 2012a, b). However, field observations (Fig. 2) indicated that there were two main patterns of alteration including the stones of the Castle of Chambord; biological colonization (different types of lichens and mosses) and stone detachment in the form of stone spalling and exfoliation.

**The Castle of Chambord: climatic conditions, temperature and relative humidity data**

The Castle of Chambord is located in an area that experiences a mild humid temperate climate with moderately warm summers and no dry season. According to meteorological data, for the period 1997–2012, gathered from Bricy Air Base weather station (Orléans, France), the nearest station to the Castle of Chambord, the temperature typically varies from 0 to 26 °C and is rarely below −5 °C or above 31 °C. The relative humidity typically ranges from 45 to 98 %, rarely dropping below 30 % and reaching as high as 100 %. Precipitation is most likely around December, occurring on 48 % of days, while it is least likely around August, occurring on 28 % of days. Typical wind speeds vary from 1 to 7 m/s, rarely exceeding 11 m/s.

**Fig. 2** Types of degradation of stones observed in the north wall of the east tower



The possibility of snow falling is highest around February, occurring on 7 % of days. This climate represents a typical environment that promotes physico-chemical weathering processes.

To estimate the risk of damage to the stones due to the variations in climatic conditions, two sets of data were acquired and analysed. The first relates to meteorological data: air temperature, air relative humidity and rainfall were recorded every 5 min for about 17 months, from April 2010 to August 2011, using the meteorological station installed on the roof of the east tower of the castle. The second set of data includes the stone temperature and relative humidity. They were measured using thermal-humidity sensors inserted into the walls of the same tower. A total of 16 sensors were set up in two directions (north and south) at three different levels (top, middle and bottom, i.e. 2 m; 5 and 8 m), on the surface and at different depths inside the stones (15, 30, 50 and 250 mm). These data were measured every 30 min for 3 years, from June 2009 to June 2012, and provide comprehensive information on the changes in temperature and moisture both on the surface and inside the stones. Figure 3 shows the east tower with a meteorological station on its roof and the sensors installed at different positions on the walls. The east tower is much damaged by weathering and has been only slightly restored (Janvier-Badosa et al. 2013). Thus, this tower represents an interesting case for the study of the relationship between climate data and stone weathering.

### Data analysis and discussion

The meteorological data, air temperature and air relative humidity, for the period 1973–2012 obtained from Bricy weather station, were analysed and compared with meteorological data obtained from the local weather station placed on the roof of the east tower of the castle. Figure 4

presents the monthly variations in mean maximum and mean minimum, both of air temperature and air relative humidity for the two periods 2010–2011 and 1973–2012. These evolutions for the two different periods are similar. Therefore, the data acquired in situ during the period 2010–2011 can be considered as representative of the local climatic conditions in the studied area.

In the present work, the methodologies followed to assess the risk of damage to the stones due to weathering can be summarized as follows:

- Analysis of the daily variation in stone surface temperature was used to assess the role of thermal stress.
- Analysis of air temperature and relative humidity was linked with analysis of stone surface temperature in an attempt to estimate the risk of physical weathering damage due to freezing and condensation on the stone surface.
- The measured values of temperature and relative humidity at different depths inside the stones together with the characterization of the pore size distribution of the studied stones were analysed to investigate the frequencies of freezing and of condensation events within the porous structure of the stones.

### Daily variation in stone/air temperature and thermal stress

The stone surface temperature (SST) of the two wall directions, north and south, of the east tower is characterized with seasonal variations over the year. Table 2 presents the extreme values of SST over 3 years, from June 2009 to June 2012. In the hot summer months, June, July and August, the SST exceeds 27 °C for the north wall, and in the case of the south wall it exceeds 34 °C. In the cold months, November to February, the temperature falls



**Fig. 3** The meteorological station above the east tower and the sensors positioned on the south wall



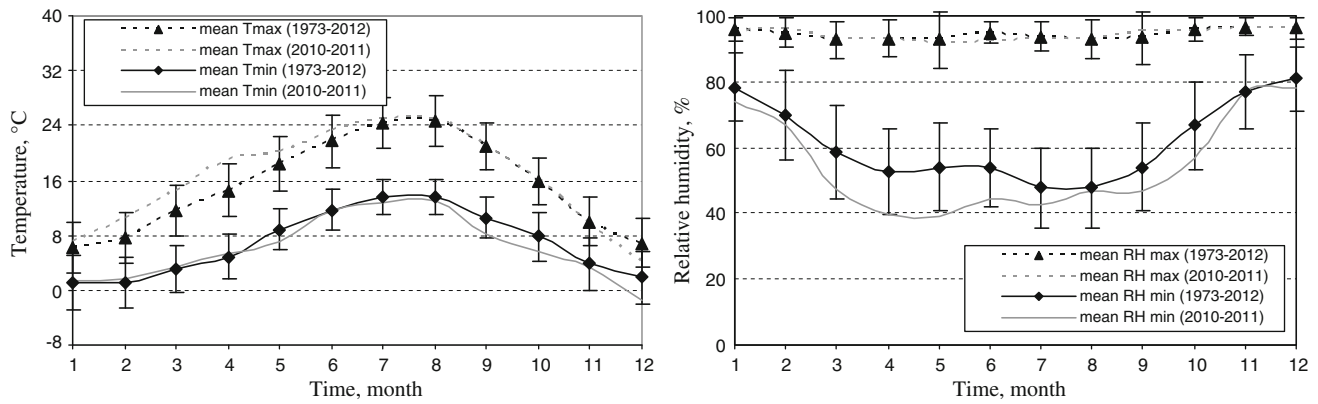


**Fig. 4** Monthly variations in the extremes values of mean air temperature (on the *left*) and mean air relative humidity (on the *right*) for the two periods: 2010–2011 and 1973–2012

**Table 2** Summary of the extreme stone surface temperature values over 3 years

Year	Highest three values of SST (°C)		Lowest three values of SST (°C)		No. of days with SST >30 °C		No. of days with SST <0 °C	
	North wall	South wall	North wall	South wall	North wall	South wall	North wall	South wall
2009/2010	28.3 (02/07)	35.9 (06/08)	-7.6 (08/01)	-8.2 (05/01)	0	47	47	46
	29.4 (21/07)	36.7 (16/08)	-7.3 (15/02)	-8.4 (08/01)				
	29.0 (19/08)	37.8 (19/08)	-7.5 (16/02)	-8.3 (15/02)				
2010/2011	29.3 (01/07)	35.3 (27/06)	-6.1 (30/11)	-6.5 (30/11)	1	37	36	41
	30.6 (02/07)	35.0 (01/07)	-3.9 (15/12)	-5.7 (14/12)				
	29.0 (09/07)	34.5 (21/08)	-4.8 (26/12)	-5.8 (26/12)				
2011/2012	27.8 (26/06)	37.4 (27/06)	-12.6 (07/02)	-14.2 (07/02)	2	29	26	25
	31.1 (27/06)	35.9 (28/06)	-11.4 (09/02)	-11.0 (06/02)				
	30.5 (28/06)	35.7 (22/08)	-10.9 (12/02)	-12.3 (09/02)				

below freezing point, with -12.6 and -14.2 °C, respectively, as the lowest SSTs for the north and south walls.

The number of days with SST higher than 30 °C ranges between 0 and 2 and 29 and 47 for the north and south walls, respectively. There are between 25 and 47 days with sub-zero temperatures for the north and south walls, respectively. Figure 5 presents the preliminary analysis of the daily variations in SST. There is a wide range of daily variations in SST, up to 13, 24 °C and down to 0.25, 0.2 °C over the year, for the north and south walls, respectively.

To provide more detailed analysis for the daily variations in SST, the maximum and minimum air temperatures for the days characterized with the highest values of SST are listed in Table 3 and compared with maximum and minimum values of SST, for the north and south walls, respectively. For the north wall the analysis shows that the maximum air temperature exceeded the maximum SST by a range of 1.56–6.5 °C. In contrast, in the case of the south wall, the maximum SST exceeded the maximum air temperature by up to 5.5 °C. Concerning the minimum temperature values, in general, the SST was slightly higher than the minimum air temperature for both wall directions.

Consequently, for the stone located in the north wall, the daily variations in air temperature are higher than the daily variations in SST by up to 3.4–9.2 °C, while in the south wall these two variations are quite similar. These findings are attributed to the effect of direct exposure to sun radiation in the case of the stones located in the south wall. This can explain why the SST after midday is higher than the surrounding air temperature, while generally, at other times, it is equal to or slightly below the air temperature.

To assess the effect of direct insolation on the heating of the stone surface, it is important to take into account the albedo. Albedo is defined as the thermal rock property that controls the amount and speed of heat absorbed by its surface due to radiation (Warke and Smith 1998). In the experimental work of Viles (2005), albedo was examined precisely for two stones: granite and marble. Resulting from the absorption of sun radiation, the granite was found to have a higher surface temperature due to its darker colour, that is, low albedo, compared with marble.

When the stones are subjected to cyclic temperature variations, the constituent minerals expand/contract in different intensities depending on their thermal expansion

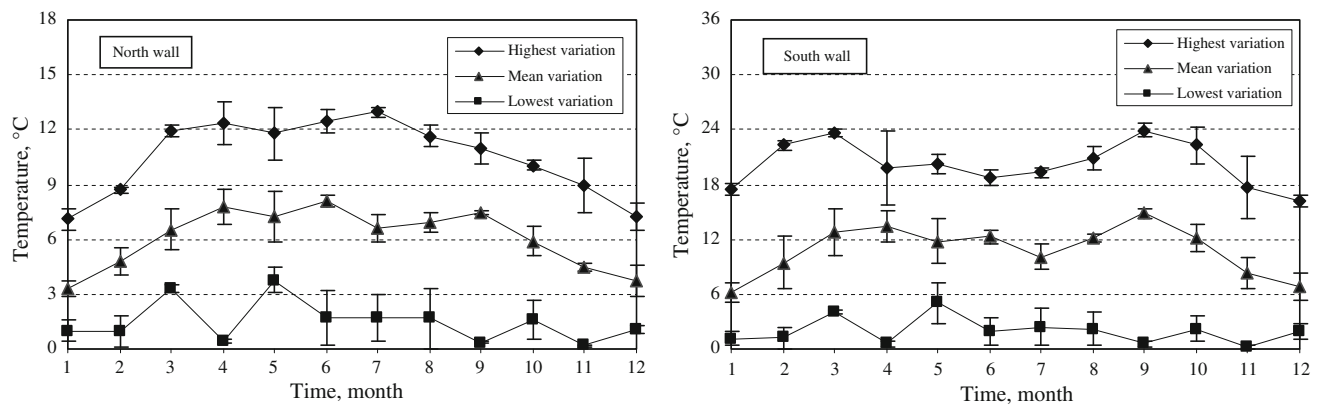


**Fig. 5** Highest, mean and lowest daily variation in stone surface temperature for the period June 2009–June 2012

**Table 3** Values of SST and air temperature at some specific days

Date (dd/mm/yy)	Max $T_{\text{air}}$ (°C)	Min $T_{\text{air}}$ (°C)	$\Delta T_{\text{air}}$ (°C)	North façade wall			South façade wall		
				Max SST (°C)	Min SST (°C)	$\Delta$ SST (°C)	Max SST (°C)	Min SST (°C)	$\Delta$ SST (°C)
27/06/2010	31.2	13.9	17.3	28.3	16.8	11.5	35.3	16.2	19.1
01/07/2010	32.5	15.1	17.4	29.3	18.2	11.1	35.0	17.9	17.1
02/07/2010	32.2	17.5	14.7	30.6	20.2	10.4	34.5	19.8	14.7
09/07/2010	33.0	19.1	13.9	29.0	21.0	8.0	31.8	20.4	11.4
26/06/2011	32.4	12.8	19.6	27.8	14.9	12.9	33.0	14.6	18.4
27/06/2011	37.0	15.6	21.4	31.1	18.0	13.1	37.4	17.8	19.6
28/06/2011	33.0	18.1	14.9	30.5	22.2	8.3	35.9	21.7	14.2
21/08/2011	31.8	13.0	18.8	25.3	15.7	9.5	34.5	15.5	19.0
22/08/2011	30.3	19.5	10.8	27.6	20.2	7.4	35.7	20.7	15.0

coefficient values; consequently, the induced internal pressure within the stones can lead to changes in the microstructures of the stones by creating new cracks or the development of the pre-existing micro-cracks (Mutlutürk et al. 2004; Yavuz et al. 2006, 2010). Temperature variation is not the only factor influencing the micro-structure of stones, but its effects are extended to induce damage to the stones on a macro scale, that is, the damage induced by thermal stress. Referring to the work of Bonazza et al. (2009b) the risk of damage due to thermal stress on Carrara marble was predicted using Eq. (1):

$$\sigma_T = \frac{E \cdot \alpha \cdot \Delta T}{1 - \nu} \quad (1)$$

where  $\sigma_T$  is the maximum thermal stress, MPa;  $E$  is the Young's modulus, MPa;  $\alpha$  is the thermal expansion coefficient,  $\text{K}^{-1}$ ;  $\Delta T$  is the daily variation in SST, K;  $\nu$  is the Poisson's ratio, %.

The thermo-mechanical properties of the studied stones, tuffeau and Richemont stone, were measured and are presented in Table 1. The daily variation in SST is calculated

as the difference between the daily maximum and minimum stone surface temperatures.

Table 4 presents the main annual percentile values of  $\sigma_T$  calculated using Eq. (1) for the data analysed over a period of 3 years, both for the north and south walls. The term percentile can, statistically, be defined as the value of a variable (e.g. thermal stress) below which a certain percentage of occurrences of observations are equal or smaller. For example, in the case of tuffeau located in the north wall, the 50th percentile of the calculated thermal stresses is  $\leq 0.23$  MPa. Again, the 100th percentile corresponds to the maximum value of the thermal stress and the 0th percentile corresponds to the minimum. To estimate the risk of damage to the stones located in the Castle of Chambord due to the effect of thermal stress, we compared the calculated thermal stress,  $\sigma_T$ , with the maximum sustainable load. The maximum sustainable loads for tuffeau and Richemont stone were obtained by adopting the same procedure used in the literature (Bonazza et al. 2009b; Ponziani et al. 2012). In this analysis, the unconfined compressive strength (UCS) value of the two stones was

**Table 4** Annual percentile values of thermal stress calculated at two façade walls of the east tower

Percentage (%)	Thermal stress (MPa)			
	Tuffeau		Richemont stone	
	North wall	South wall	North wall	South wall
0	0.04	0.04	0.11	0.12
1	0.05	0.07	0.16	0.20
5	0.09	0.11	0.26	0.35
25	0.17	0.26	0.51	0.80
50	0.23	0.42	0.71	1.29
75	0.30	0.58	0.94	1.80
82	0.34	0.65	1.05	1.98
95	0.41	0.78	1.26	2.39
99	0.46	0.86	1.42	2.64
100	0.49	0.91	1.52	2.79

divided by a safety factor of three. The values of the UCS of the studied stones are presented in Table 1. The maximum sustainable loads are 3.89 MPa for tuffeau and 6.47 MPa for Richemont stone.

The results presented in Table 4 illustrate that all the calculated values of thermal stress for Richemont stone are three times higher than those calculated for tuffeau. Such behaviour can be attributed to the different values of the thermo-mechanical properties (Young’s modulus, Poisson’s ratio and the thermal expansion coefficient) of the two stones. Also, the values of the thermal stresses are always higher for the south wall compared to the north wall, for both types of stone. These findings can be attributed to the fact that the south wall is more exposed to direct sunlight. Moreover, tuffeau located in the south wall have a maximum thermal stress of 0.91 MPa compared with 0.49 MPa for the same type of stones in the north wall, while in the case of Richemont stone, these stresses are 2.79 and 1.52 MPa for the south and north walls, respectively. On the other hand, the results show that the risk of damage to the two studied stones, located in the walls of the north façade or the south façade, from thermal stress is probably negligible, where all values of thermal stress never exceed the maximum sustainable load of the stone.

**Condensation**

Water movement can induce severe damage due to the dissolution of stone minerals, reduction of the free energy of grain material weakening the resistance, transport of the air pollutants into porous media, and so on. The most common sources of moisture are rainfall, capillary water and condensation. The role of condensation in the wetting

of stones and its effects on the degradation of stones as a microclimate process have been studied in the literature (Camuffo and Sturaro 2001; De Freitas and Schmekal 2003; Ponziani et al. 2012).

The dew point temperature ( $T_d$ ) is the temperature at which the free water vapour, in humid air at constant barometric pressure, turns from a gaseous to a liquid state and finally accumulates on the cold material surfaces. At 100 % relative humidity, the  $T_d$  is equivalent to air temperature. The  $T_d$  can be calculated using Eq. (2) based on the August–Roche–Magnus approximation for the saturation vapour pressure of water in air as a function of temperature.

$$T_d = \frac{b\gamma(T, RH)}{a - \gamma(T, RH)} \tag{2}$$

with

$$\gamma(T, RH) = \frac{aT}{b + T} + \ln\left(\frac{RH}{100}\right)$$

where  $RH$  relative humidity;  $100 > RH > 1$ , %;  $T$  air temperature,  $60 > T > 0$ , °C;  $a$  17.271;  $b$  237.7 °C.

Air relative humidity plays a significant role in promoting the process of condensation. To assess the occurrence of condensation on the surface of the studied walls, the first step was to analyse precisely the relative humidity of the air surrounding the Castle of Chambord. The data analysis of mean air relative humidity, obtained from the meteorological station installed on the roof of the east tower of the Castle of Chambord, for the period April 2010 to August 2011 shows that the values of mean air relative humidity are, mostly, between 60 and 90 %. They reach values exceeding 95 % in the winter months and rarely fall below 50 %. Again, the analysis shows that the mean air relative humidity reaches up to 96–98 % in the high humidity months, October–January, while it falls down to 48–53 % in the less humid months, April, June and July. A considerable number of days are characterized with high

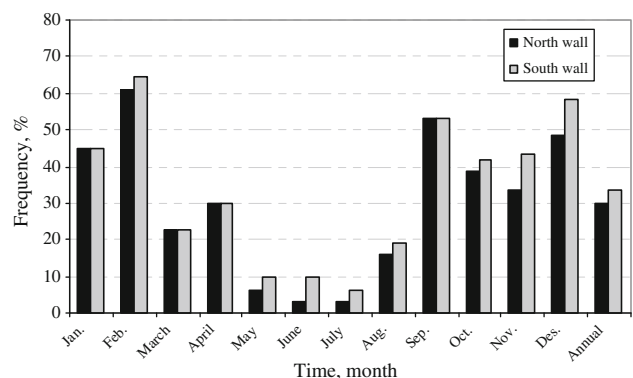


**Fig. 6** Frequency of condensation events on stone surfaces of north and south walls

humidity: 14.2 % of days per year experience air relative humidity of over 90 %, and only 2.5 % of days per year to air relative humidity of <55 %. We can conclude that the Castle of Chambord is located in an area that experiences a high to moderate humid climate which can enhance the availability of moisture within the stones. As tuffeau is characterized with high water holding capacity (Table 1), we can raise the hypothesis: in situ, the observed degradation of tuffeau in the Castle of Chambord may be related, strongly, to characteristics of the humid climate.

The work presented in this study focused on examining the action of condensation in the degradation of the stones from two different base methods: first, through condensation on the external stone surfaces; and second, through condensation within the porous structure of the stones (i.e. taking into consideration the meniscus curvature of the pore water). The following paragraphs present these two approaches.

#### Condensation on the stone's surface

The procedure followed to assess the condensation occurrence on the stone's surface consists of comparing the

calculated  $T_d$  with SST. When  $T_d$  is higher than SST, the water vapour condenses on the stone's surface. The frequencies of condensation events on stone surfaces, both on north and south walls of the east tower, were calculated and are presented in Fig. 6. These events occur throughout the year with annual frequencies exceeding 29 and 33 % for the north and south façade walls, respectively. They are more frequent in September–February. On the other hand, the frequencies for the south wall are slightly higher compared with the north walls; this can be attributed, as mentioned in “Daily variation in stone/air temperature and thermal stress”, to the fact that stones in the south wall experience higher variations in daily surface temperature, thus enhancing the probability of  $T_d$  being greater than the SST.

#### Condensation within the stone porous structure

In the case of the porous material and within the micro-pore system, the condensation phenomenon is governed by Kelvin's law, where for each pore radius ( $r$ ) there is a critical relative humidity,  $RH_c$  (Camuffo 1998). Condensation occurs when the measured relative humidity inside

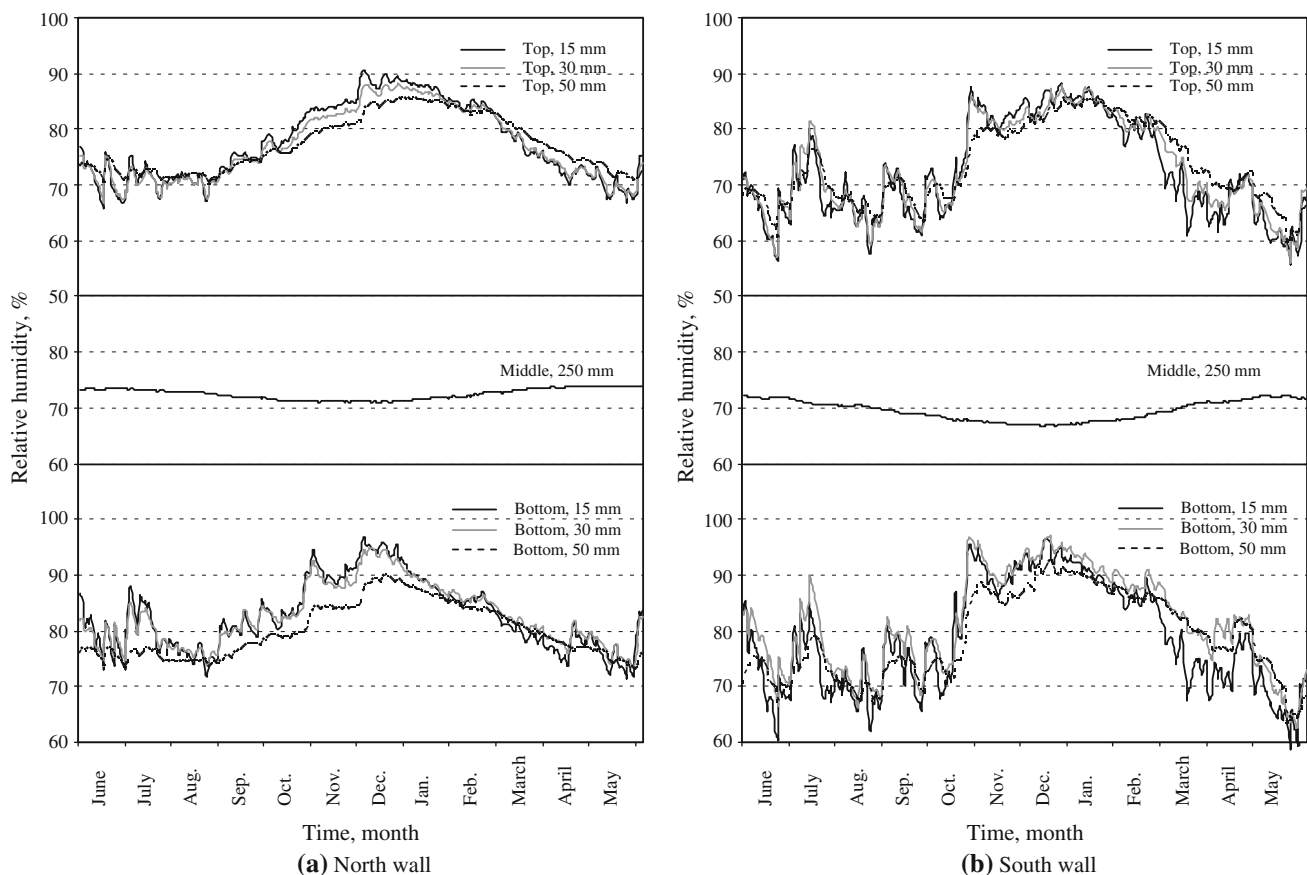


**Fig. 7** Evolution of mean maximum relative humidity at different depths inside the stone for the period of 3 years: **a** north wall, and **b** south wall



the stone ( $RH_s$ ) is higher than the calculated  $RH_c$ . The  $RH_c$  can be calculated using Eq. (3):

$$RH_c = 100 \cdot e^{\frac{-2\sigma_w \cdot V_m}{r \cdot RT}} \quad (3)$$

where  $\sigma_w$  surface tension of water in air–liquid interaction, 0.072 N/m;  $V_m$  molar volume of water, 18 cm<sup>3</sup>/mol;  $R$  gas constant, 8.3144621 N m/mol/K;  $T$  temperature of thermodynamic system in equilibrium, K.

Figure 7 presents the evolution of the mean maximum  $RH_s$  measured for a period of 3 years using thermal–humidity sensors inserted into the walls of the east tower in different directions (north and south), at different levels (top, middle and bottom) and at different depths inside the stones (15, 30, 50 and 250 mm). Both for the north and south walls, the mean maximum  $RH_s$  inside the bottom stones is higher than the mean maximum  $RH_s$  inside the top stone. The measured mean maximum  $RH_s$  inside the bottom stones ranges between 70 and 95 %, compared with 60 and 90 % for the top stones. There is a slight fluctuation in depth with the mean maximum  $RH_s$  values measured near the surface (i.e. 15, 30 and 50 mm). At 250 mm depth, the mean maximum  $RH_s$  is more stable with values between 65 and 75 % both for the north and south walls. Finally, because the stones in the south wall are more subjected to sun radiation, the measured humidity inside these stones experiences fluctuations of greater amplitude compared to stones in the north wall.

The calculated values of  $RH_c$  are listed in Table 5. These values mainly depend on the pore size radius, with a limited effect of temperature. Indeed, for a full range of SST experienced in the field, there is no significant variation in the calculated values of  $RH_c$ . The resulting variation is small enough to be ignored compared to sensor accuracy. Hence, in this analysis, a constant mean value of the temperature of the stones in each case was used to calculate the  $RH_c$ . The effect of meniscus curvature of the pore water in micro-pores can be observed through the reductions in the  $RH_c$  values for smaller pore radii. In this study, the measured  $RH_s$  were analysed and compared with  $RH_c$ . As for thermal stress, the frequency of condensation events was estimated using a percentile format, and the annual frequencies of days with condensation occurrences (i.e. values of  $RH_s$  higher than the  $RH_c$ ) are presented in Table 5 as a function of pore radius.

The results show that the frequencies of condensation depend on the height of the stone in the wall (top or bottom), the depth within the stone (15, 30, 50 and 250 mm) and the orientation of the wall façade (north or south). Stones located at the bottom are always subjected to more frequent condensation events than those at the top. The annual frequencies of condensation events mainly depend on the depth inside the stone. For stones located on the

**Table 5** Annual frequencies of condensation events with values of  $RH_c$  as a function of pore radius at different locations on the north and on the south walls

Pore radius, $r$ ( $\mu\text{m}$ )	$RH_c$ (%)	North wall						South wall								
		Bottom of the wall		Middle		Top of the wall		Bottom of the wall		Middle		Top of the wall				
		15 mm depth	30 mm depth	50 mm depth	250 mm depth	15 mm depth	30 mm depth	50 mm depth	15 mm depth	30 mm depth	50 mm depth	250 mm depth	15 mm depth	30 mm depth	50 mm depth	
1	99.891	0.1	–	–	–	–	–	0.2	–	–	–	–	–	–	–	–
0.1	98.915	3.4	0.3	–	–	–	–	2.5	3.1	–	–	–	0.1	–	–	–
0.09	98.795	4.2	0.9	–	–	–	–	2.6	3.8	–	–	–	0.1	–	–	–
0.07	98.454	4.8	1.9	–	–	–	–	3.2	4.9	–	–	–	0.1	–	–	–
0.05	97.842	5.6	2.7	–	–	–	–	4.0	6.7	0.1	–	–	0.2	–	–	–
0.03	96.430	7.2	3.9	–	–	0.6	–	5.7	9.0	0.6	–	–	0.3	0.4	–	–
0.01	89.666	18.6	14.5	4.9	–	4.5	4.3	23.1	30.6	10.6	–	–	2.3	3.1	–	–
0.009	88.586	21.8	17.7	7.2	–	5.7	4.8	26.9	36.0	13.7	–	–	3.9	4.1	0.1	–
0.007	85.571	36.7	35.4	14.4	–	16.3	12.1	37.4	47.5	31.3	–	–	11.3	8.4	3.4	–
0.006	83.378	48.2	48.5	26.5	–	29.8	20.4	44.3	54.8	40.8	–	–	20.5	15.7	10.4	–
0.005	80.401	62.4	61.1	42.9	–	40.6	39.2	50.8	62.6	51.2	–	–	31.5	31.9	27.2	–
0.003	69.636	93.9	97.6	98.8	95.4	82.6	83.2	74.6	81.9	79.2	44.8	–	58.9	61.2	62.8	–

north wall, the condensation occurrences always decrease with depth. In contrast, for the south wall, the percentages of condensation events are maximal at 30 mm depth. This could be attributed to the impact of direct sunlight on the humidity of the stones near the surface. However, there is no condensation at 250 mm depth, even for the shortest pore radii. For 30 and 50 mm depths inside the stones, the condensation events for the bottom part of the south wall face are more frequent compared with north at the same height. On the other hand, for the top part of the north wall face, these occurrences are equal or slightly higher compared with the south.

The annual frequencies of condensation events inside the porous structures of the stones have been correlated to the results obtained from the mercury porosimetry test. The porosimetry analysis indicated that Richemont stone has a pores size distribution restricted to the range 0.01–2  $\mu\text{m}$  of the pore radius with the main peak of incremental pore volume at 1  $\mu\text{m}$  with a shouldering at 0.3  $\mu\text{m}$  (see Fig. 2). Taking into account Table 5, only in a few days per year the Richemont stone is submitted to condensation. In accordance with the observed smallest pores in Richemont stone, the higher frequencies of condensation events reach

up to 18.6 and 30.6 % for the bottom part of the north and south walls, respectively. These occurrences are much lower or nil for the same pore sizes at other levels or at different depths within the stones. On the other hand, the pore network of tuffeau is characterized by a typically bimodal distribution with a large mean peak at 4  $\mu\text{m}$  (from pore radius of 0.003–10  $\mu\text{m}$ ) and the second one at 0.005  $\mu\text{m}$ . The smallest pores are notably subjected to condensation. The frequencies of condensation for the pore radius of 0.003  $\mu\text{m}$  range, respectively, between 93.9–98.8 and 74.6–81.9 % at the bottom part of the north and south walls at different depths within the stones. Therefore, as tuffeau in the Castle of Chambord is subjected to a high occurrence of condensation, this physical process may be considered to be one of the main causes for the degradation of this stone.

#### Freezing–thawing action

When stone is in a moist state and undergoes variations in temperature around freezing point, it may be subjected to freezing. Several experimental works conducted on different stone types have shown that their physical and

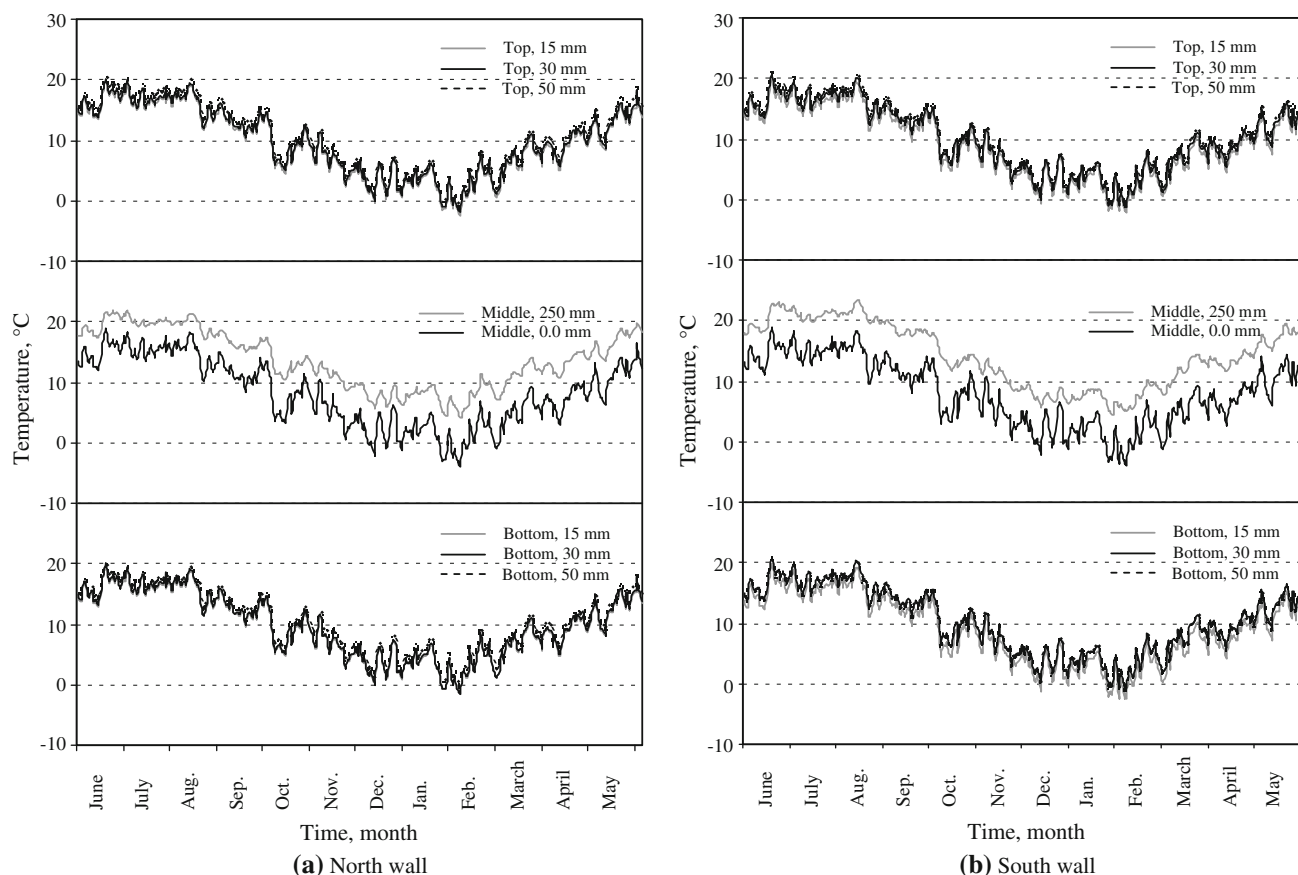


**Fig. 8** Evolution of mean minimum temperature at stone surface and at different depths inside the stone for a period of 3 years: **a** north wall, and **b** south wall

engineering properties are widely influenced by the recurrent action of freezing–thawing (Altindag et al. 2004; Mutlutürk et al. 2004; Tan et al. 2011; Yavuz et al. 2006).

To assess the risk of freezing damaging the stones in the Castle of Chambord, the frequencies of days with freezing–thawing events were evaluated. As for condensation, the freezing events both on the stone surface and within the pore network of the stone were included in the analysis. The effect of the meniscus curvature of the pore water leads to the lowering of the freezing point temperature,  $T_{FP}$ , for smaller pores (Camuffo 1998). The  $T_{FP}$  can be calculated using the expression below:

$$T_{FP} = -273 \frac{2\sigma_{sl}}{r \cdot P_s L_f} \tag{4}$$

where  $\sigma_{sl}$  surface tension at solid–liquid interface, 32.1E–03 N/m;  $p_s$  ice density, 0.917 g/cm<sup>3</sup>;  $L_f$  latent heat fusion, 333.55 N m/g.

Figure 8 presents the evolution of the mean minimum temperature on the stone surface and at different depths inside the stone for the period of 3 years, both for the north and south walls. The mean minimum temperatures measured on the stone surface and at different depths inside the stone (15, 30 and 50 mm) are quite similar and range between 0.0 and 20 °C. They fall below 0.0 °C in the months of January and February. These observations are independent of the orientation and the height of the stones. However, in the case of the 250 mm depth, the mean minimum temperatures never drop below 0.0 °C.

To estimate the frequencies of days with freezing–thawing events, we refer to the comparison between the calculated  $T_{FP}$  with the measured minimum stone temperature. Freezing is assumed to happen when the minimum stone temperature is below the  $T_{FP}$ .

*Freezing action on the stone surface*

On the stone surface,  $T_{FP}$  was assumed to be 0.0 °C, and the freezing events were observed in two ways: the first by analysing the minimum SST measured using thermal–humidity sensors for the period of 3 years (from June 2009 to June 2012). The data analysis showed that the annual frequencies of freezing events were 9.7 and 10.5 % for the south and north walls, respectively (see Table 6). It should be noted that freezing events were assumed to happen when the SST was just below the  $T_{FP}$ , regardless of the presence of water on the stone surfaces. The second analysis was conducted over only a short period, from 1 April 2010 to 25 August 2011, (i.e. the period of the meteorological data acquisition using the local weather station). The objective of this second analysis was to identify the conjunction between freezing events and the presence of water on the stone surface due to rain or condensation.

**Table 6** Annual frequencies of freezing events with values of  $T_{FP}$  as a function of pore radius at different locations on the north and on the south walls

Pore radius, $r$ ( $\mu\text{m}$ )	$T_{FP}$ , (°C)	South wall														
		North wall						South wall								
		Bottom of the wall		Middle		Top of the wall		Bottom of the wall		Middle		Top of the wall				
1	-0.03	5.8	5.7	3.8	0.2	6.2	5.7	4.7	4.7	7.7	5.4	4.7	0.1	6.7	5.5	5.1
0.1	-0.29	5.2	5.1	3.5	0.1	5.8	5.5	4.4	4.4	7.2	4.9	4.6	0.1	6.1	5.2	4.5
0.09	-0.32	5.1	5.1	3.5	0.1	5.7	5.4	4.4	4.4	7.1	4.8	4.5	0.1	6.0	5.1	4.4
0.07	-0.41	4.9	5.0	3.3	0.1	5.6	5.2	4.1	4.1	6.9	4.7	4.5	-	5.8	5.0	4.3
0.05	-0.58	4.8	4.7	3.1	0.1	5.5	4.8	3.8	3.8	6.3	4.5	4.1	-	5.7	4.5	3.9
0.03	-0.97	3.9	3.7	2.8	-	4.7	4.2	2.8	2.8	5.8	3.8	3.4	-	5.2	3.8	3.3
0.01	-2.90	1.9	1.8	1.2	-	2.1	1.7	1.4	1.4	4.6	2.1	1.7	-	2.6	1.9	1.5
0.009	-3.22	1.7	1.7	1.1	-	1.8	1.5	1.2	1.2	2.6	1.8	1.3	-	2.3	1.6	1.4
0.007	-4.14	1.3	1.2	0.8	-	1.4	1.2	0.7	0.7	2.1	1.1	0.9	-	1.7	1.1	1.0
0.006	-4.83	1.0	1.0	0.4	-	1.0	0.7	0.7	0.7	1.6	0.9	0.7	-	1.2	0.9	0.8
0.005	-5.80	0.7	0.6	0.2	-	0.7	0.6	0.5	0.5	1.0	0.5	0.4	-	1.0	0.5	0.5
0.003	-9.40	-	-	-	-	0.1	0.1	-	-	0.2	-	-	-	0.1	0.1	-

At stone surfaces the  $T_{FP}$  is zero and the corresponding annual freezing events are 9.74 and 10.49 % for the north and south walls, respectively

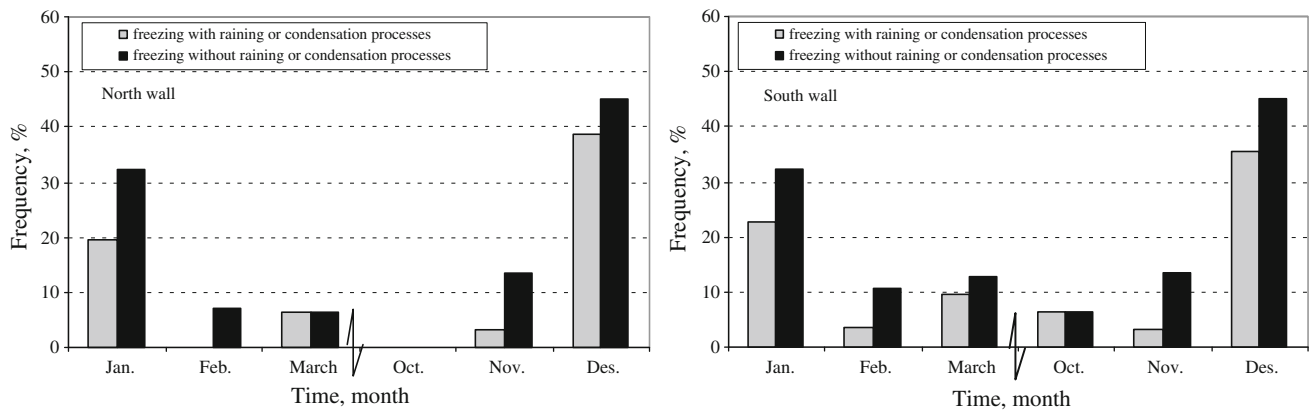


**Fig. 9** Frequency of freezing events with or without effects of raining and condensation processes

Figure 9 presents the frequencies for each month. Freezing events only occur during the period November–March and are more concentrated in December and January. Freezing occurrences are more frequent for the south wall compared to the north. A comparison between both types of analysis was made to assess the interest of taking into account the presence of condensed water on the stone surface. The result indicates that considering the presence of water significantly reduces the calculated frequencies of freezing (see Fig. 9). Hence, the first analysis focuses on estimating the risk of damage due to freezing, while the frequencies of this weathering process are actually measured in the second analysis.

#### *Freezing action within the stone's porous structure*

Concerning the freezing action within the porous structure of the stone, the frequencies of freezing events over the period of 3 years were estimated by analysing the values of the minimum stone temperatures measured at different depths inside the stone, at different levels (top, middle and bottom) on the south and north walls. Again, the percentile format was used to present the results of the analysis, and the annual frequencies of freezing events are presented in Table 6. As described in Eq. (4), the values of the freezing point temperature, within the porous structure of the stone, depend on pore radius; consequently, the  $T_{FP}$  drops for the pores with smaller radii.

From the results of the mercury porosimetry test, in combination with the results presented in Table 6, it is evident that the two limestones, tuffeau and Richemont stone, can be considered as exposed to similar magnitudes of freezing–thawing. The results revealed that the location of the stones (on the top or at the bottom of the walls) has a limited effect on the annual frequencies of freezing events. However, freezing occurrences are slightly higher at 15 and 30 mm compared to 50 mm depths, and

nil at 250 mm. In general, the south wall is a bit more exposed to freezing events compared to the north wall.

#### **Conclusion and outlook**

In this study, statistical analysis concerning the temperature and humidity of stones located in the walls of the east tower of the Castle of Chambord, together with meteorological data of the weather experienced at the castle, was taken into consideration to estimate the role of climatic conditions in the development of degradation of two French limestones, tuffeau and Richemont stone, used in the construction and restoration of the castle. The study focused on the estimation of the stones' behaviour with respect to three weathering processes: thermal stress, condensation and freezing–thawing.

The SST analysis shows that the daily variations in stone temperature can reach 20 °C. However, the daily variation depends on the orientation of the stone in the studied tower: higher variation is detected in the south wall, which is exposed to the sun, compared to the north wall. The effects of thermal stress generated by daily variations in temperature are more significant in the Richemont stones than in tuffeau. Indeed, even if the mechanical strength of Richemont stone is higher compared with tuffeau, tuffeau is less stiff (lower Young's modulus) and can experience higher deformation due to thermal dilation without damage. However, all calculated values of thermal stress remain lower than the maximum sustainable load for both stones. As a consequence, daily variations in temperature may not be considered to be a significant source of degradation. However, cyclic fluctuations in temperature over time may generate stone damage by fatigue, but this last aspect was not investigated in this study.

Relative humidity data show that the Castle of Chambord is located in an area that experiences a high to

moderate humid climate, which can enhance the continuous availability of moisture within the stones. The presence of biological colonization (more than 43 % of all identified alterations) on the east tower of the Castle of Chambord confirms the humid climate that reigns in situ. Condensation events occur on stone surfaces throughout the year, with annual frequencies exceeding 29 and 33 % for the north and south façade walls, respectively. The frequencies of condensation events analysed with sensor measurements in the walls of the east tower show that stones located at the bottom are subjected to more frequent condensation events than those at the top. The occurrence of condensation decreases with depth inside the stone. At the 250 mm depth, no condensation occurs. This is due to fluctuations in relative humidity decreasing with depth until 250 mm, where the relative humidity is almost constant. The frequency of condensation for Richemont stone hardly reaches 30 %, while it reaches even higher than 90 % for tuffeau. This is due to the effect of pore size distribution, much finer for tuffeau compared to Richemont stone.

No freezing is experienced at the 250 mm depth. Freezing occurrence is maximal near the surface (at 30 and 15 mm depths) and slightly lower at the 50 mm depth. The height and the orientation of the stones have no significant effects. However, freezing frequency is low and concerns only the porosity limited to the finest pores.

As a conclusion, the analysis of the Chambord data indicated that neither Richemont stone nor tuffeau is affected by thermal stress, while condensation events are more frequent in tuffeau. The risk of freezing for both stones is similar, but is not considered to be the main damaging process. In this study, the measured stone temperature and stone humidity were analysed by a simplified approach. Thus, it is recommended that more attention be given to water saturation when assessing freezing action, and to investigate the role of rainfall, drizzle, fog, hail and snow, in combination with wind direction. Finally, cyclic effects must be studied to assess the damage generated by fatigue.

## References

- Altindag R, Alyildiz IS, Onargan T (2004) Mechanical property degradation of ignimbrite subjected to recurrent freeze–thaw cycles. *Int J Rock Mech Min Sci* 41:1023–1028
- Beck K, Al-Mukhtar M (2005) Multi-scale characterization of two French limestones used in historic constructions. *Int J Restor Build Monum* 11(4):219–226
- Bonazza A, Messina P, Sabbioni C, Grossi CM, Brimblecombe P (2009a) Mapping the impact of climate change on surface recession of carbonate buildings in Europe. *Sci Total Environ* 407:2039–2050
- Bonazza A, Sabbioni C, Messina P, Guaraldi C, De Nuntiis P (2009b) Climate change impact: mapping thermal stress on Carrara marble in Europe. *Sci Total Environ* 407:4506–4512
- Brunetaud X, De Luca L, Janvier-Badosa S, Beck K, Al-Mukhtar M (2012a) Application of digital techniques in monument preservation. *Eur J Environ Civil Eng* 16(5):543–556
- Brunetaud X, Stefani C, Janvier-Badosa S, Beck K, Al-Mukhtar M (2012b) Comparison between photomodelling and laser scanning to create a 3D model for a digital health record. *Eur J Environ Civil Eng* 16(sup1):s48–s63
- Camuffo D (1998) *Microclimate for cultural heritage*. Elsevier, Amsterdam
- Camuffo D, Sturaro G (2001) The climate of Rome and its action on monument decay. *Climate Res* 16:145–155
- De Freitas CR, Schmekal A (2003) Condensation as a microclimate process: measurement, numerical simulation and prediction in the Glowworm cave, New Zealand. *Int J Climatol* 23:557–575
- Eklund S (2008) Stone weathering in the monastic building complex on Mountain of St Aaron in Petra, Jordan. M.Sc Thesis, University of Helsinki-Finland
- Hoxha D, Do D, Belayachi N (2010) A fully coupled thermo-hydro mechanical analysis of the impact of temperature and humidity variation on the state of historical stone buildings. In: 8th international symposium on the conservation of monuments in the Mediterranean Basin, Patras
- Janvier-Badosa S, Beck K, Brunetaud X, Al-Mukhtar M (2010) Characterization of stone weathering: A case study for Chambord Castle, France. In: 8th international symposium on the conservation of monuments in the Mediterranean Basin, Patras
- Janvier-Badosa S, Beck K, Brunetaud X, Al-Mukhtar M (2013) Historical study of Chambord Castle: basis for establishing the monument health record. *Int J Archit Herit* 7:247–260
- Moropoulou A, Theoulakis P, Chrysophakis T (1995) Correlation between stone weathering and environmental factors in marine atmosphere. *Atmos Eng* 29:895–903
- Mutlutürk M, Altindag R, Türkc G (2004) A decay function model for the integrity loss of rock when subjected to recurrent cycles of freezing–thawing and heating–cooling. *Int J Rock Mech Min Sci* 41:237–244
- Ponziani D, Ferrero E, Appolonia L, Migliorini S (2012) Effects of temperature and humidity excursions and wind exposure on the arch of Augustus in Aosta. *J Cult Herit* 13:462–468
- Pope GA, Meierding TC, Paradise TR (2002) Geomorphology's role in the study of weathering of cultural stone. *Geomorphology* 47:211–225
- Tan X, Chen W, Yang J, Cao J (2011) Laboratory investigation on the mechanical properties degradation of granite under freeze–thaw action. *Cold Reg Sci Technol* 68:130–138
- Van TT, Beck K, Al-Mukhtar M (2007) Accelerated weathering tests on two highly porous limestones. *Environ Geol* 52(2):283–292
- Viles HA (2005) Microclimate and weathering in the central Namib Desert, Namibia. *Geomorphology* 67:189–209
- Warke PA, Smith BJ (1998) Effect of direct and indirect heating on the validity of rock weathering simulation studies and durability tests. *Geomorphology* 22:347–357
- Yavuz H, Altindag R, Sarac S, Ugur I, Sengun N (2006) Estimating the index properties of deteriorated carbonate rocks due to freeze–thaw and thermal shock weathering. *Int J Rock Mech Min Sci* 43:767–775
- Yavuz H, Demirdag S, Caran S (2010) Thermal effect on the physical properties of carbonate rocks. *Int J Rock Mech Min Sci* 47:94–103